J Appl Electrochem (2008) 38:457–468
DOI 10.1007/s10800-007-9459-1

ORIGINAL PAPER

An investigation of copper interconnect deposition bath ageing by electrochemical impedance spectroscopy

C. Gabrielli · P. Moçotéguy · H. Perrot · D. Nieto-Sanz · A. Zdunek

Received: 22 January 2007 / Revised: 16 November 2007 / Accepted: 21 November 2007 / Published online: 11 December 2007

Abstract Electrochemical impedance spectroscopy was performed on copper interconnect plating baths during deposition to study their degradation (ageing). A kinetic-based model was used to simulate the impedance scans by taking into account the organic additives in the reaction mechanism. Also, an equivalent circuit analysis was performed to characterize the deposition process in terms of resistive and capacitive components. Experimental results for two chemistries indicate that the low-frequency impedance relaxations change as the plating bath ages. Impedance diagrams calculated from the kinetic model resulted in a reasonable fit with the experimental impedance scans. In addition, the low-frequency capacitive and inductive impedance loop diameters are proposed as parameters to follow bath ageing. From these results, a monitoring method is proposed which could be applied to an industrial production line.

Keywords Copper · Electrodeposition · Damascene process · Microelectronics · Ageing · Impedance

C. Gabrielli (✉) · P. Moçotéguy · H. Perrot
UPR 15 CNRS, LISE, Univ. P. et M. Curie, 4 place Jussieu, Boite 133, 75252 Paris, France
e-mail: cg@ccr.jussieu.fr

D. Nieto-Sanz
Air Liquide, Centre de Recherche Claude Delorme, 78354 Jouy en Josas, France

A. Zdunek
Air Liquide, Chicago Research Center, Countryside, IL 60525, USA

1 Introduction

Dual-damascene copper electroplating is now commonly used for depositing copper to produce ultra-thin metal interconnects in integrated circuit (IC) semiconductor manufacturing. The copper electroplating baths used in the dual damascene process contain a mixture of H_2SO_4 and $CuSO_4$, to which chloride ions and different types of organic additives are added. The organic additives are brightener/accelerator, inhibitor/suppressor, and leveller types of compounds that allow superconformal filling to occur in the high depth/width ratio interconnect trenches and vias without voids or defects in the deposit [1, 2]. Specifically, the brighteners are propane sulfonic acid derivatives such as MPSA ($HSO_3-(CH_2)_3-SH$) or SPS ($HSO_3-(CH_2)_3-S-S-(CH_3)_2-SO_3H$). They change the nucleation process by providing growth sites and accelerate the charge transfer process at the copper interface. The suppressors are polyalkylene glycols ($HO-(C_kH_{2k}-O)_n-H$). They adsorb evenly at the wafer surface, change the deposit structures, and increase the overpotential. Since the accelerator additives can diffuse more easily than the inhibitor molecules into the bottom of the trenches, higher deposition rates occur at the bottom of the trench and bottom-up, "superconformal" filling is achieved without voids in the deposit. Levellers are used to decrease the copper growth rate at regions with high mass transfer rates, thereby limiting the thickness of the copper deposit above the trenches and vias and reducing the amount of overplating [2].

Electrochemical impedance spectroscopy (EIS) has previously been used to investigate copper deposition without additives. In addition to the expected high frequency capacitance loop due to charge transfer resistance, low frequency capacitive and inductive relaxations have also been observed [3, 4]. The low frequency capacitive

relaxations are due to either the surface coverage of a reaction intermediate when diffusion is not the rate limiting process, or a slow removal of either an anionic species, a hydroxide or organic molecule from the surface [4–6]. In addition, previous investigations of copper deposition revealed that electrode activation occurs with increasing current density and that the low frequency features from EIS appear to be strongly dependent on the growth mode of the copper deposit [7–10].

Gabrielli et al. [10], investigated the role of chlorides in the copper deposition mechanism using a kinetic model combined with EIS measurements on copper plating baths without organic additives. At sufficiently high current densities, the kinetic model showed that the surface concentration of CuCl is the dominant species on the electrode surface, supporting the major role of a CuCl to Cu metal deposition reaction pathway. Gabrielli et al. [11] also used EIS to investigate the kinetics of a "reference" copper deposition bath containing additives that are known in literature to provide superfilling in submicrometer cavities. The reference bath consists of a non-proprietary mixture containing specific amounts of the various inorganic components ($CuSO_4$, H_2SO_4, Cl) and organic additives (MPSA and PEG) [1]. Gabrielli et al. formulated a kinetic model taking into account the competitive adsorption of the inhibitor polyethylene glycol (PEG) and the accelerator mercapto propanesulfonic acid (MPSA), as well as reduction of the resulting reaction intermediates. Model predictions for the shape of the impedance diagrams during copper deposition were in good agreement with actual EIS impedance diagrams not only for freshly-made copper bath solutions, but also for aged baths; plating baths where copper was deposited for long periods and that experienced additive depletion and degradation [12].

In practice, the dual-damascene process for integrated circuit manufacturing uses commercial plating baths rather than the reference bath described above to achieve superfilling. These industrial plating baths are proprietary, where the inorganic concentrations (sulfuric acid, copper sulfate and chloride) are known but the exact compositions of the organic additives are not explicitly revealed to the end users, except as volumetric concentrations of an additive "concentrate". For instance, the accelerator additive concentration is often reported as mL of accelerator A concentrate per L of plating bath volume.

Thus, the objective of this work was twofold. First, a kinetic-based model similar to the model previously proposed by Gabrielli for a reference plating bath [11, 12] was formulated and EIS experiments performed to determine if the reaction mechanism associated with industrial, dual-damascene copper deposition baths would have the same mechanistic structure as the reference plating bath. Secondly, since characteristic shapes of the EIS diagrams were consistently observed for these plating baths, certain parameters of the scans were proposed as markers of the bath ageing process to better quantify the additive degradation process, with the ultimate goal of devising a sensor to determine when the plating bath needs replenishment due to additive degradation.

2 Kinetic-based model for industrial plating baths

It is assumed in the proposed model that the copper plating bath contains copper sulfate, sulfuric acid, chloride ions, and two organic additive entities, an accelerator (Acc) and inhibitor/suppressor (Inh). The accelerator and inhibitor entities may or may not be a single chemical species (possible multiple accelerator or suppressor chemistries due to the proprietary nature of the additives) but, for modelling purposes, they are each considered to behave as a single species.

Similarly to the reference bath described previously, the cathodic deposition of copper in sulfuric acid solution is believed to occur through two consecutive charge transfer steps involving the soluble intermediate Cu^+ [13–17]:

$$Cu^{2+} + (*) + e^- \xrightarrow{k_1} Cu^+(*) \quad (1)$$

$$Cu^+(*) + e^- \xrightarrow{k_2} Cu \quad (2)$$

The two-steps reaction pathway with adsorbed CuCl as intermediate is also taken into account since Cl^- ions are present in the plating bath:

$$Cu^{2+} + Cl^- + e^- + (*) \xrightarrow{k_3} CuCl(*) \quad (3)$$

$$CuCl(*) + e^- \xrightarrow{k_4} Cu^0 + Cl^- + (*) \quad (4)$$

In addition, the adsorption of the inhibitor, Inh, is followed by the reduction of the reaction intermediate:

$$Inh + CuCl(*) \xrightarrow{k_5} Inh{-}Cl{-}Cu^I(*)) \quad (5)$$

$$Inh{-}Cl{-}Cu^I(*) + e^- \xrightarrow{k_6} Cu^0 + Inh^* + Cl^- \quad (6)$$

where Inh* is a degraded form of Inh with a lower molecular mass due to the breaking of the chains of the Inh polymer.

The proposed model also assumes that a Cu^IAcc complex forms spontaneously in the bulk bath since the compounds needed for its existence are simultaneously present in the plating bath. Indeed, according to the value of the equilibrium constant of the Cu^+ disproportionation reaction reported by Koh et al. [2], the concentration of free Cu^+ can be calculated as 3.74×10^{-4} M when $[Cu^{2+}] = 0.25$ M. This value is far above the usual accelerator concentration of approximately 10^{-5} M. Thus, the complex is most likely in

equilibrium with its constituents according to the reaction below and is always present in the plating bath even at concentrations where it cannot be detected.

$$Cu^{+} + Acc \leftrightarrows Cu^{I}Acc \tag{7}$$

$$\frac{\Delta\theta_1}{\Delta E} = T_1 = \frac{K_1 + k_3c_0c_1\left(\frac{b_6k_6\theta_2}{j\omega+k_6}\left(1+\frac{k_7c_3}{j\omega+k_8+k_7c_3}\right)+\frac{b_8k_8\theta_3}{j\omega+k_8+k_7c_3}\right)}{j\omega + k_3c_0c_1 + k_4 + k_5c_2 + k_3c_0c_1\left(\frac{k_5c_2}{j\omega+k_6}+\frac{k_7c_3}{j\omega+k_8+k_7c_3}\left(1+\frac{k_5c_2}{j\omega+k_6}\right)\right)} \tag{13}$$

This reaction has an equilibrium constant:

$$K_{f,Cu^{I}Acc} = \frac{[Cu^{I}Acc]}{[Cu^{+}][Acc]} \Leftrightarrow [Cu^{I}Acc] = K_{f,Cu^{I}Acc}[Cu^{+}][Acc] \tag{8}$$

Previous results from the reference plating bath model revealed that the inductive loop in the EIS scan was directly associated with the surface coverage of the Cu^{I}-accelerator complex. It was shown that the surface coverage of this complex increases as its concentration in the bath increases, no matter what the inhibitor or accelerator concentration are in the bath [11]. Thus, a similar reaction mechanism can be written for the industrial plating bath model, where it is assumed that the complex $Cu^{I}Acc$ adsorbs at the copper surface according to the following equation:

$$Cu^{I}{-}Acc + (*) \xrightarrow{k_7} Cu^{I}{-}Acc(*) \tag{9}$$

It is also assumed that, once adsorbed, the complex is reduced according to the following reaction:

$$Cu^{I}{-}Acc(*) + e^{-} \xrightarrow{k_8} Cu^{0}{-}Acc \tag{10}$$

where Cu^{0}–Acc defines the accelerator species trapped in the copper deposit.

From reactions (1)–(6), (9) and (10), the impedance Z_F, was calculated according to the following equation:

$$Z_F^{-1} = \frac{\Delta I_F}{\Delta E} = R_t^{-1} + \beta F[(k_4 - c_0(k_1 + k_3c_1))T_1 + (k_6 - c_0(k_1 + k_3c_1))T_2 + (k_8 - c_0(k_1 + k_3c_1))T_3] \tag{11}$$

where

$$R_t^{-1} = \beta F[c_0(b_1k_1 + b_3k_3c_1)(1 - \theta_1 - \theta_2 - \theta_3 - \theta_{Cu^{+}}) + b_2k_2\theta_{Cu^{+}} + b_4k_4\theta_1 + b_6k_6\theta_2 + b_8k_8\theta_3] \tag{12}$$

c_0, c_1, c_2, and c_3 are the concentrations of Cu^{2+}, Cl^{-}, Inh–Cl–Cu^{I}, and Cu^{I}–Acc, respectively, $\theta_{Cu^{+}}$, θ_1, θ_2, and θ_3 are the surface coverage's of Cu^{+}, CuCl, Inh–Cl–Cu^{I}, and Cu^{I}–Acc, respectively.

Finally, the change in surface coverage with the change in potential can be rewritten as:

$$\frac{\Delta\theta_2}{\Delta E} = T_2 = \frac{-b_6k_6\theta_2 + k_5c_2T_1}{j\omega + k_6} \tag{14}$$

$$\frac{\Delta\theta_3}{\Delta E} = T_3 = -\frac{b_8k_8\theta_3 + k_7c_3(T_1 + T_2)}{j\omega + k_8 + k_7c_3} \tag{15}$$

These equations are used to calculate real and imaginary impedance values at different frequencies ranging from 0.001 Hz (1 mHz) to 100,000 Hz, the practical range of frequencies used in electrochemical impedance spectroscopy. The complete development of the reference bath model and the details of the calculations on which this model is based are given elsewhere [11].

3 Experimental

Industrial copper plating baths from Enthone-OMI (ATMI) containing sulfuric acid, copper sulfate and chlorides (termed the virgin makeup solution (VMS)), were used for the plating and EIS measurements. The plating baths also contained a proprietary mixture of accelerator, suppressor and leveller additive species. The volumetric concentrations of the additives in the VMS are specified by the manufacturer and given as $mL_{additive}/L_{plating\ solution}$. Thus, for example, to achieve the correct accelerator mixture concentration in the plating bath, the recommended volume of the accelerator liquid concentrate was added to the VMS. The volumetric concentrations of the different additives can be measured by techniques such as cyclic voltammetric stripping, however, the exact chemistry and concentrations of the specific compounds in each of the additive mixture concentrates are not known by the end-user. Two industrial baths, called "Chemistry I" and "Chemistry II" were used in the experiments. Chemistry I was a relatively older copper plating bath used for depositing copper interconnects for >90 nm IC geometries. Chemistry II was a newer bath for which superconformal

copper deposition up to a depth/width ratio of 10 for 90–65 nm IC geometries can be achieved.

The two plating baths were aged by depositing copper in a plating test cell for a given length of time and charge, and the degradation of the bath during the ageing process was followed by electrochemical impedance spectroscopy. Bath ageing was quantified in these experiments using an ageing term with units of A h L^{-1}. This bath ageing term was obtained by multiplying the current by the plating time to obtain the amount of coulombs passed with the bath, and then dividing by the volume of the plating bath. The ageing experiments (plating/measurement) were performed with a 0.7 L solution and a set-up containing two independent electrical circuits. First, a copper plating circuit to age the bath was used which consisted of a phosphorized copper anode plate from Metal Samples containing 0.024% w/w of P, a 99.9% industrial-grade copper cathode acting as the deposition substrate, and a saturated mercurous sulfate electrode (SSE). Copper was plated in the plating bath at 16 mA cm^{-2} which is a typical copper deposition current density for this application. Both anode and cathode active areas were controlled using a TFM Electromask green insulating resin (supplied by Henkel) and fixed at 63.75 cm^2. The experimental conditions described here are identical with those used earlier [12]. Secondly, an electrochemical characterization circuit was used in the same cell which contained an additional saturated mercurous sulfate electrode, a copper anode sheet whose material was identical to the one used in the anode ageing circuit, and a copper rotating disk electrode rotating at 2000 rpm. In addition to the plating cell setup described here, Chemistry II was also tested in a plating cell that contained a separator between the anode and cathode. Details of this setup are described in [12].

For all measurements, the rotating disk electrode consisted of a 5 mm diameter copper disc (Goodfellow 99.99% + copper rod embedded in an inert and insulating Presi Allylic Glass Fiber resin). The copper disk was polished with 1200 grade SiC paper and rinsed with deionised water to clean the surface before each measurement. Its active area was 0.2 cm^2. The impedance spectra were measured using a Solartron 1250 frequency response analyzer during ageing. Data acquisition was performed using a software program designed by the CNRS/LISE laboratory. The EIS spectra were acquired in a frequency range of 62.5 kHz down to 10 mHz, in galvanostatic mode with an imposed DC deposition current density of 25 mA cm^{-2} (Sotelem-Vinci PGstat-Z). The magnitude of the AC current was chosen in order that the potential perturbation was lower than 10 mV peak to peak. It was necessary to stop the measurements at 10 mHz in the low frequency range since the impedance measurements lasted 20 min at this frequency range (including 4 min for the stabilization of the current), and therefore the measurement circuit actually contributed to bath ageing by about 0.4 A h L^{-1}. For measurements at lower frequencies, the measurement time would have been much longer (e.g. 2.5 to 3 h for measurements down to 1 mHz), leading to excessive ageing of the bath and causing drifts in the impedance scan, which would have been incompatible with impedance measurements of good quality.

4 Results and discussion

4.1 EIS during ageing of the plating bath

Figures 1–3 show the evolution of the impedance diagram during ageing of Chemistry I, Chemistry II, and Chemistry II with the separator plating cell. Copper plating was performed to give bath ageing amounts ranging between 10 and 16 A h L^{-1}. Similar to results obtained from the reference bath [11], the impedance diagrams for these chemistries generally show four relaxation loops. Three capacitive loops were often observed where the high frequency loop is related to the charge transfer resistance in parallel on the double layer capacity, and the intermediate frequency loop should be related to the CuCl reaction intermediate. In the low frequency range, capacitive and inductive loops appear that can be ascribed to the various organic additives in the plating bath.

The impedances given in Figs. 2 and 3 at the beginning of ageing, are similar to that observed for the reference bath, where the third capacitive loop is relatively small. This is also similar to the impedance observed when the concentration of the accelerator is increased in fresh reference baths [11]. However, the aged industrial baths based on Chemistry I, exhibit a larger third capacitive loop. For Chemistry II with plating cell separator (Fig. 3), the third capacitive loop and the inductive loop increase greatly with ageing. On the other hand, for Chemistry I, both the third capacitive loop and the inductive loop decrease and then start to increase after bath ageing has reached a specific time. It is interesting to note that the two capacitive loops found in the high frequency range did not change with bath ageing for all the tested chemistries. Only the third capacitive loop and the inductive loop varied with time.

4.2 Deposition kinetics during bath ageing

The impedance diagrams plotted during the ageing of Chemistry I, Chemistry II, and Chemistry II with separator were fitted using the kinetic-based impedance model. The calculated impedance diagrams are plotted on Figs. 1–3 for

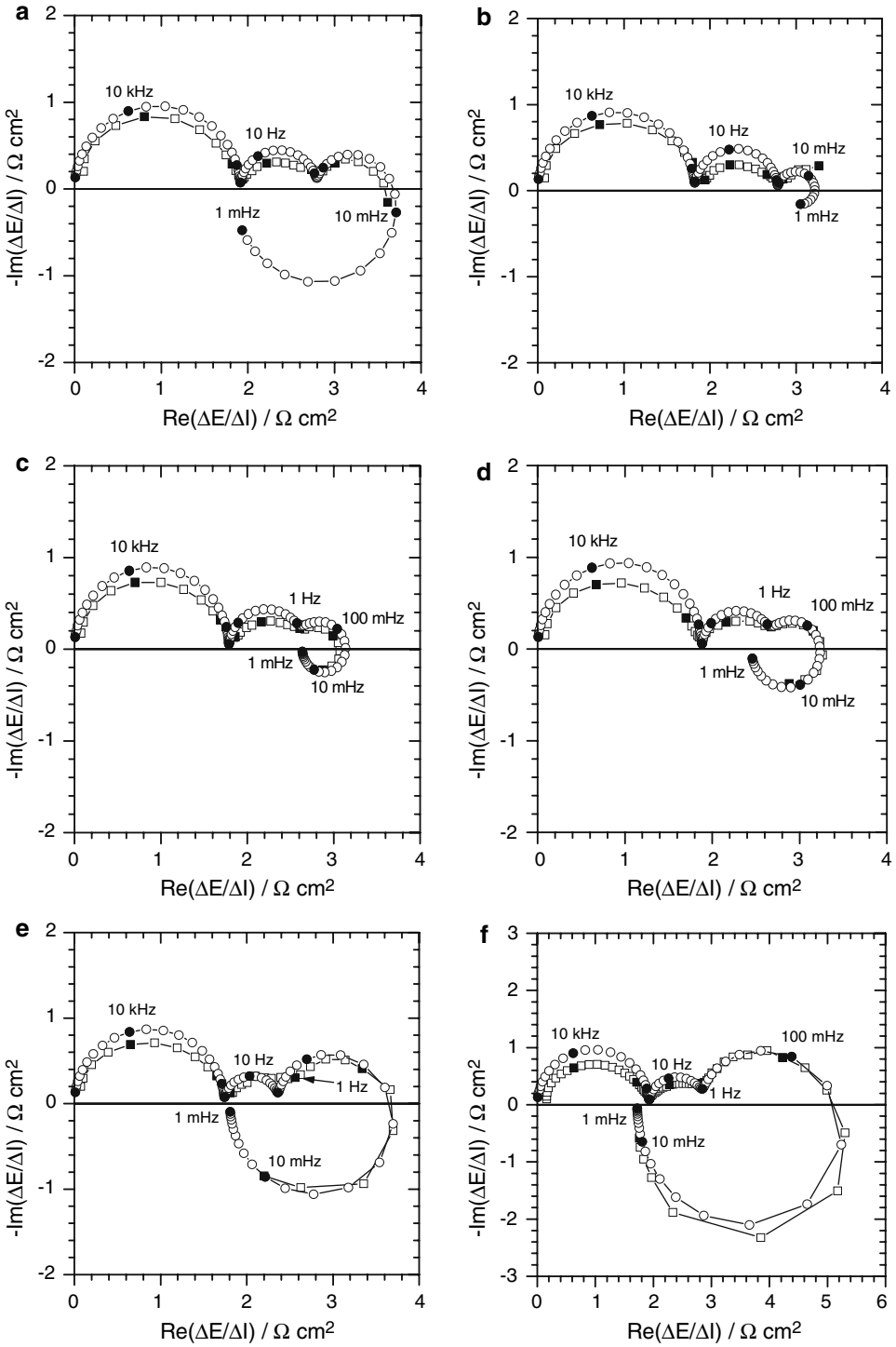

Fig. 1 Evolution of the impedance diagram during ageing with Chemistry I; experimental impedance diagrams (□), calculated impedance diagrams (○); solid circles and squares indicate the frequency decades from 10 kHz to 0.01 Hz for experiments and 0.001 Hz for calculations. The age of the plating bath is indicated by the quantity of electricity per volume unit which has passed through the plating cell I t V^{-1} = (**a**) 0.19 A h L^{-1}, (**b**) 2.59 A h L^{-1}, (**c**) 7.11 A h L^{-1}, (**d**) 8.44 A h L^{-1}, (**e**) 12.1 A h L^{-1}, (**f**) 16 A h L^{-1}

equivalent amounts of bath ageing. The parameters used to fit the experimental data are given in Tables 1–3. The parameters k_1, k_2, k_3, and k_4 remain fairly constant during bath ageing, except for Chemistry II with a separator where k_3 is ten times lower than the value obtained for Chemistry I and Chemistry II without a separator. The main differences in the parameters occur with those associated with the inhibitor and accelerator complex species.

Further analysis can be performed using the fitted parameter values. Since the k_5c_2 and k_7c_3 cannot be separated and if we assume that the rate constants k_5 and k_7 are constant during ageing, these lumped parameters represent the concentrations c_2 and c_3 of Inh and the complex Cu^{I}–Acc, respectively. Figure 4 shows the change in inhibitor and accelerator complex concentrations for Chemistry I during bath ageing. The inhibitor concentration

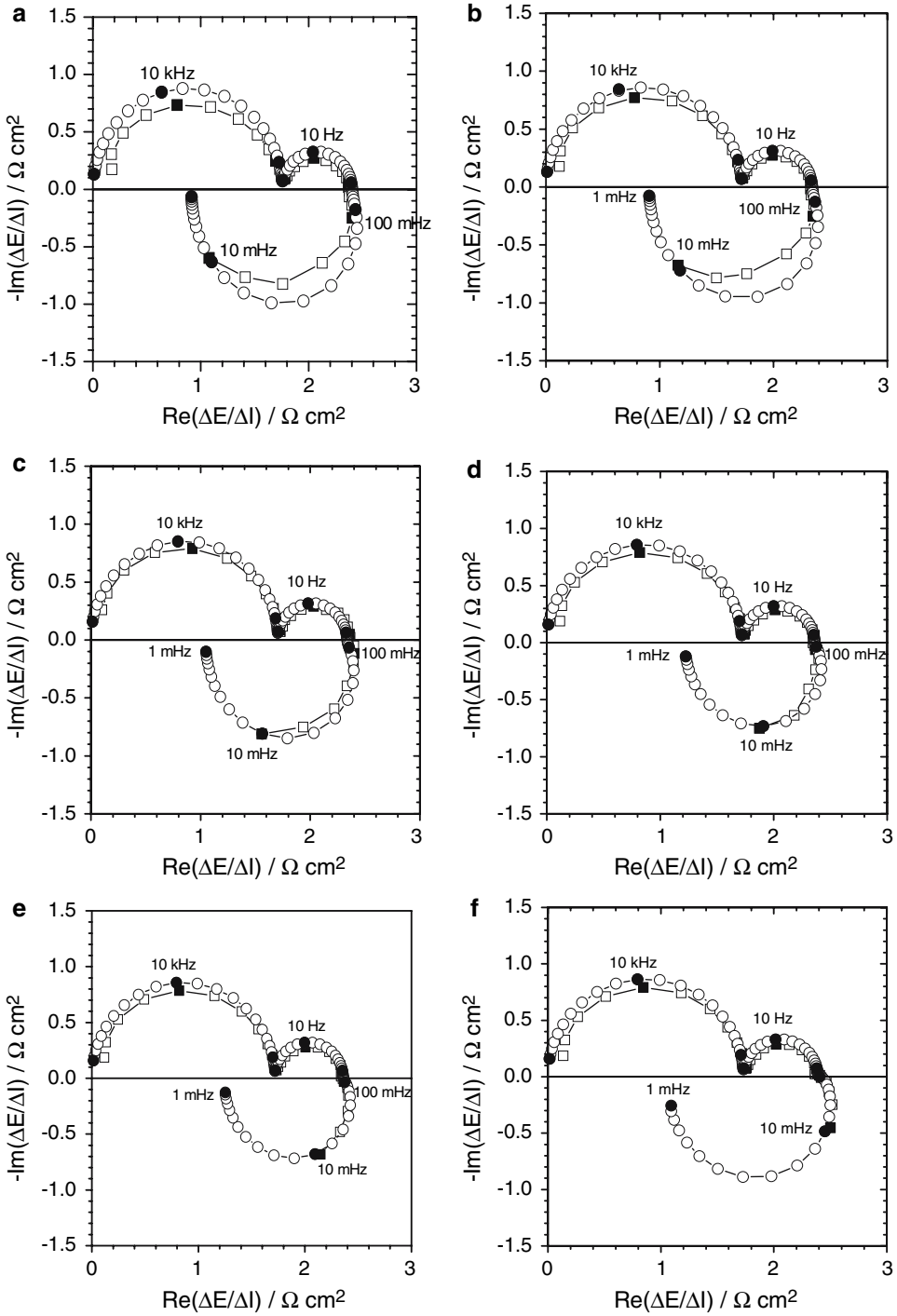

Fig. 2 Evolution of the impedance diagram during ageing with Chemistry II; experimental impedance diagrams (□), calculated impedance diagrams (○); solid circles and squares indicate the frequency decades from 10 kHz to 0.01 Hz for experiments and 0.001 Hz for calculations. The age of the plating bath is indicated by the quantity of electricity per volume unit which has passed through the plating cell I t V^{-1} = (**a**) 0.21 A h L^{-1}, (**b**) 2.96 A h L^{-1}, (**c**) 7.71 A h L^{-1}, (**d**) 9.5 A h L^{-1}, (**e**) 10.78 A h L^{-1}, (**f**) 11.95 A h L^{-1}

stays relatively constant at the electrode surface, whereas the accelerator complex concentration decreases with ageing. This is the same behaviour as observed for the reference bath. Figure 5 represents the concentration of the conjectured inhibitor and the accelerator complex concentrations for Chemistry II with and without the separator in the plating cell. It is obvious from this plot that the separator changes the kinetics of copper deposition. The Inh concentration only increases slightly, but this may be due to fitting difficulties which were observed in the calculations. However, the accelerator concentration decreases quickly in presence of the separator as ageing proceeds whereas when the separator is not operative the accelerator concentration increases. This suggests that the separator hinders the formation of the accelerator complex or favours its degradation. However, without the separator, there is a slight decrease in concentration initially; however, the trend is for both c_2 and c_3 to increase with bath ageing.

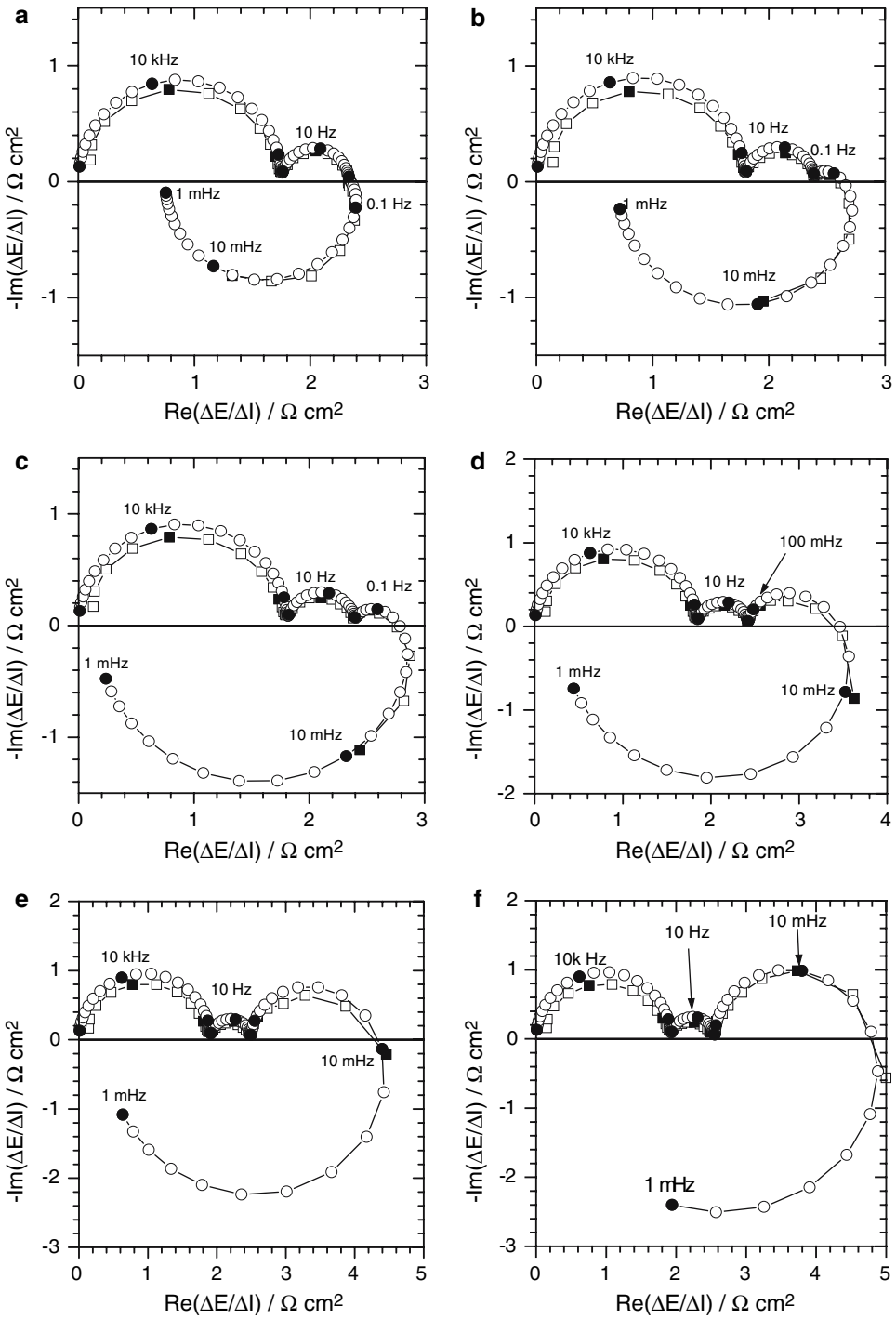

Fig. 3 Evolution of the impedance diagram during ageing with Chemistry II with a separator between the anode and cathode; experimental impedance diagrams (□), calculated impedance diagrams (○); solid circles and squares indicate the frequency decades from 10 kHz to 0.01 Hz for experiments and 0.001 Hz for calculations. The age of the plating bath is indicated by the quantity of electricity per volume unit which has passed through the plating cell I t V^{-1} = (**a**) 0.24 A h L^{-1}, (**b**) 1.54 A h L^{-1}, (**c**) 2.32 A h L^{-1}, (**d**) 3.06 A h L^{-1}, (**e**) 3.88 A h L^{-1}, (**f**) 9.94 A h L^{-1}

4.3 Characteristic impedance parameters during ageing

One of the aims of this study was to find parameters from the impedance measurements which quantitatively characterize bath ageing. As a first step, practical quantities which depend on the conditions of the experiments can be extracted from the measured impedance diagrams and are defined as:

$$DL = R_{\max} - R_{0.01}$$

$$DC = R_{\max} - R_1$$

where the parameters *DL* and *DC* are approximately the size of the inductive and third capacitive loops from the experimental diagrams, respectively. The value of *DC* is close to the diameter of the third capacitive loop, but *DL* can be different than the exact diameter of the inductive

Table 1 Parameters of the model for Chemistry I during ageing corresponding to Fig. 1

Q (AhL^{-1})	k_{10} ($cm\ s^{-1}$)	b_1 (V^{-1})	k_{20} ($cm\ s^{-1}$)	b_2 (V^{-1})	k_{30} ($cm\ s^{-1}$)	b_3 (V^{-1})	k_{40} ($cm\ s^{-1}$)	b_4 (V^{-1})	k_5c_2 ($mol\ s^{-1}\ cm^{-2}$)	k_{60} ($cm\ s^{-1}$)	b_6 (V^{-1})	k_7c_3 ($mol\ s^{-1}\ cm^{-2}$)	k_{80} ($cm\ s^{-1}$)	b_8 (V^{-1})
0.21	4.4×10^4	−10	6×10^4	−10	2.5×10^3	−16	5×10^{-3}	−10	5.75×10^{-2}	3.25×10^{-3}	−6	6.5×10^{-2}	1.75×10^{-5}	−20
2.96	4.5×10^4	−10	6×10^4	−10	2.5×10^3	−16	5×10^{-3}	−10	5.75×10^{-2}	3.25×10^{-3}	−6	5.35×10^{-2}	1.75×10^{-5}	−20
7.71	4.35×10^4	−10	6×10^4	−10	2.5×10^3	−16	5×10^{-3}	−10	5.75×10^{-2}	3.25×10^{-3}	−6	3.5×10^{-2}	3.2×10^{-5}	−20
9.5	4.3×10^4	−10	6×10^4	−10	2.5×10^3	−16	5×10^{-3}	−10	5.75×10^{-2}	3.25×10^{-3}	−6	2.5×10^{-2}	4.2×10^{-5}	−20
10.78	4.3×10^4	−10	6×10^4	−10	2.5×10^3	−16	5×10^{-3}	−10	5.75×10^{-2}	3.25×10^{-3}	−6	2×10^{-2}	3.6×10^{-5}	−20
11.95	4.17×10^4	−10	6×10^4	−10	2.5×10^3	−16	5×10^{-3}	−10	5.75×10^{-2}	3.25×10^{-3}	−6	1.2×10^{-2}	1×10^{-5}	−20

Table 2 Parameters of the model for Chemistry II without a separator between the anode and cathode during ageing corresponding to Fig. 2

Q (AhL^{-1})	k_{10} ($cm\ s^{-1}$)	b_1 (V^{-1})	k_{20} ($cm\ s^{-1}$)	b_2 (V^{-1})	k_{30} ($cm\ s^{-1}$)	b_3 (V^{-1})	k_{40} ($cm\ s^{-1}$)	b_4 (V^{-1})	k_5c_2 ($mol\ s^{-1}\ cm^{-2}$)	k_{60} ($cm\ s^{-1}$)	b_6 (V^{-1})	k_7c_3 ($mol\ s^{-1}\ cm^{-2}$)	k_{80} ($cm\ s^{-1}$)	b_8 (V^{-1})
0.24	4.45×10^4	−10	5×10^4	−10	2.5×10^3	−16	5×10^{-3}	−10	5.75×10^{-2}	3.25×10^{-2}	−6	4.5×10^{-2}	1.75×10^{-5}	−20
1.54	3.21×10^4	−10	5×10^4	−10	3.35×10^3	−16	7.5×10^{-3}	−10	5.5×10^{-2}	3.75×10^{-1}	−6	2.75×10^{-2}	1.25×10^{-5}	−20
2.32	4.3×10^4	−10	5×10^4	−10	2.75×10^3	−16	4×10^{-3}	−10	5×10^{-2}	3.25×10^{-1}	−6	1.75×10^{-2}	6×10^{-7}	−20
3.06	4.75×10^4	−10	5×10^4	−10	6.75×10^3	−20	4.5×10^{-3}	−10	5×10^{-2}	4×10^{-3}	−6	8×10^{-3}	1.25×10^{-7}	−20
3.88	6.7×10^4	−10	5×10^4	−10	7×10^3	−20	5×10^{-3}	−10	4.75×10^{-2}	4.5×10^{-3}	−6	4×10^{-3}	1.25×10^{-7}	−20
9.94	6.5×10^4	−10	7.5×10^4	−10	8×10^3	−20	4×10^{-3}	−10	8.75×10^{-2}	3.5×10^{-3}	−6	0.5×10^{-3}	0.1×10^{-7}	−20

Table 3 Parameters of the model for Chemistry II with a separator during ageing corresponding to Fig. 3

Q (AhL^{-1})	k_{10} (cm s^{-1})	b_1 (V^{-1})	k_{20} (cm s^{-1})	b_2 (V^{-1})	k_{30} (cm s^{-1})	b_3 (V^{-1})	k_{40} (cm s^{-1})	b_4 (V^{-1})	k_5c_2 (mol s^{-1} cm^{-2})	k_{60} (cm s^{-1})	b_6 (V^{-1})	k_7c_3 (mol s^{-1} cm^{-2})	k_{80} (cm s^{-1})	b_8 (V^{-1})
0.19	4.7×10^4	−10	4.9×10^4	−10	5×10^2	−16	6×10^{-3}	−10	4.75×10^{-2}	1×10^{-3}	−15	5×10^{-3}	3×10^{-7}	−20
2.59	10.7×10^4	−10	12.9×10^4	−10	8×10^2	−16	5×10^{-3}	−10	3.75×10^{-2}	1×10^{-3}	−15	0.5×10^{-3}	1×10^{-5}	−20
7.11	1.3×10^4	−10	0.9×10^4	−10	3.5×10^2	−16	20×10^{-3}	−10	4.75×10^{-2}	12×10^{-3}	−15	12×10^{-3}	29×10^{-7}	−20
8.44	1.25×10^4	−10	0.8×10^4	−10	3.5×10^2	−20	20×10^{-3}	−10	4.75×10^{-2}	12×10^{-3}	−15	7×10^{-3}	11×10^{-7}	−20
12.1	7.7×10^4	−10	7.5×10^4	−10	8×10^2	−20	5×10^{-3}	−10	5.75×10^{-2}	4×10^{-3}	−15	25×10^{-3}	0.16×10^{-7}	−20
16	4.5×10^4	−10	10×10^4	−10	7×10^2	−20	5×10^{-3}	−10	8.75×10^{-2}	6.65×10^{-3}	−15	60×10^{-3}	25×10^{-7}	−20

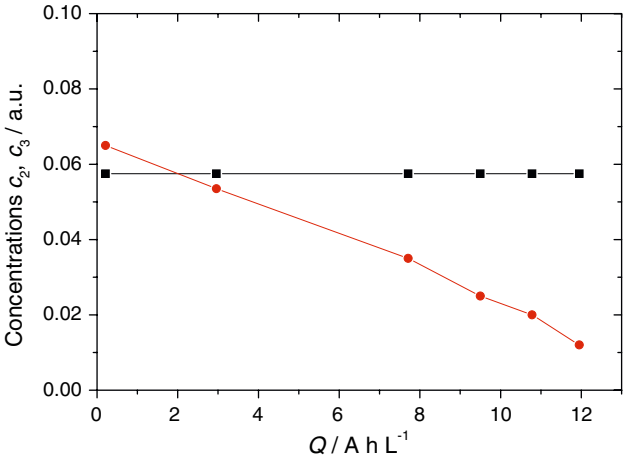

Fig. 4 Evolution of the bulk concentrations of the inhibitor c_2 (■) and the accelerator complex c_3 (●) in arbitrary units for Chemistry I

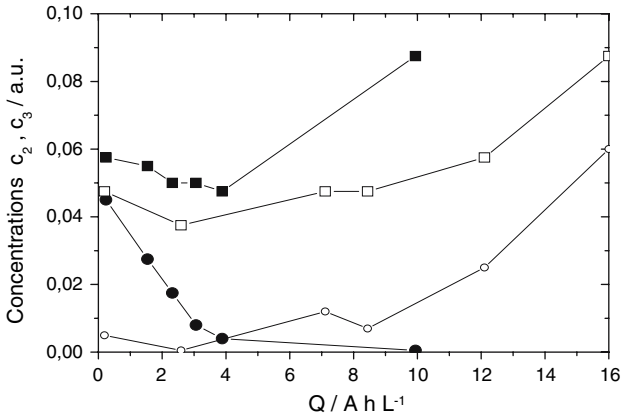

Fig. 5 Evolution of the bulk concentrations of the inhibitor c_2 (■, □) and the accelerator complex c_3 (●, ○) in arbitrary units for Chemistry II with (■, ●) and without (□, ○) separator between the anode and cathode

loop because, in general, the impedance diagram does not reach the real axis at 0.01 Hz due to the processes involved in copper deposition with additives being quite slow.

Hence, other parameters can be also obtained from the calculated impedance diagrams, which simulate the impedance down to 0.001 Hz:

$$DL_{\text{th}} = R_{\max} - R_{0.001} \qquad DC_{\text{th}} = R_{\max} - R_1$$

where $R_{\max} = \text{Max}[\text{Re}(Z(\omega))]$, $R_{0.01} = \text{Re}(Z(0.01\text{ Hz}))$, $R_{0.001} = \text{Re}(Z(0.001\text{ Hz}))$, $R_1 = \text{Re}(Z(1\text{ Hz}))$.

Figures 6–9 present the change of the parameters DL, DL_{th}, DC, and DC_{th}, when the third capacitive loop appears, during bath ageing for Chemistry I and with and without the separator for Chemistry II. Figure 6 shows the change of DL with and without a separator with respect to the accelerator complex concentration obtained from the model for Chemistry II. Figure 8 shows the change of DL and DL_{th} with respect to the bath ageing amount for

Chemistry II without separator. The two parameters decrease when the bath is aged. The experimental *DL* is more sensitive to bath ageing than DL_{th} obtained from the model, which does not change much with bath ageing. For Chemistry II without separator, there is no *DC* value to plot as the third capacitive loop is almost non-existent.

For Chemistry II with a separator, the changes in *DC*, *DL*, and DL_{th} are shown in Fig. 9. The size of the third capacitive loop increases when the bath is aged. On the other hand, the calculated inductive loop diameter, DL_{th}, increases with ageing whereas the experimental derived quantity, *DL*, decreases as the processes responsible for this loop are slowed when the bath is aged.

For Chemistry I, the three quantities, *DC*, DC_{th}, and DL_{th}, initially decrease and then increase as the bath is aged, as seen in Fig. 7 whereas *DL* increases only as it is practically equal to zero at the beginning of the experiment. The same type of behaviour was observed experimentally in the literature [18, 19]. The observed minimum was shown to correspond to the smoothest copper deposit obtained after some incubation time. Rougher deposits were observed after further bath ageing. Consequently, these quantities might be further used to obtain an estimation of the concentration of the accelerator complex.

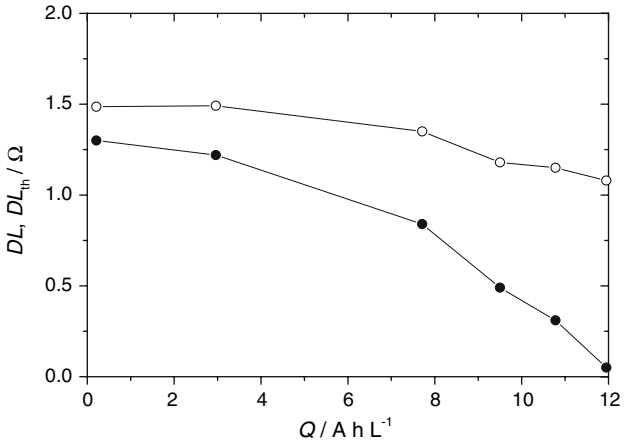

Fig. 8 Change of $DL = R_{max} - R_{0.011}$ (●) derived from experiments and $DL_{th} = R_{max} - R_{0.001}$ (○) derived from the model for Chemistry II without a separator between the anode and cathode

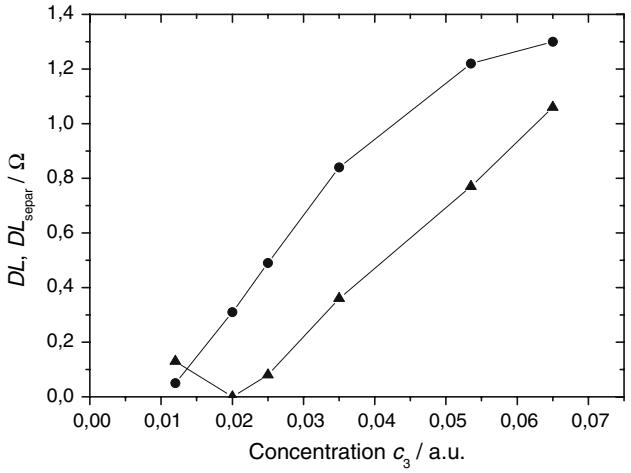

Fig. 6 Change of $DL = R_{max} - R_{0.01}$ derived from experiments for Chemistry II with (▲) and without (●) separator with respect to the concentration of the accelerator deduced from the model

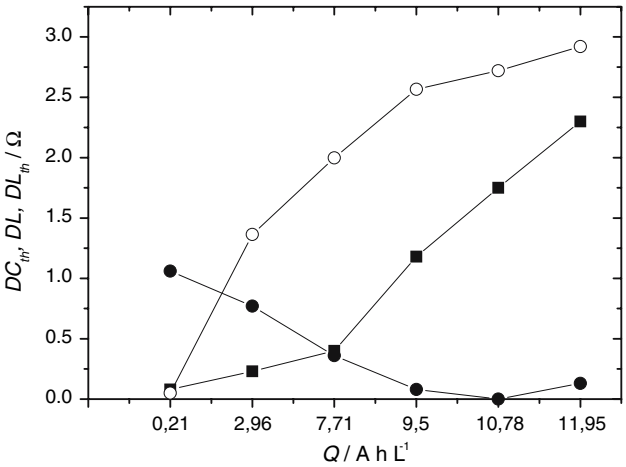

Fig. 9 Change of $DL = R_{max} - R_{0.01}$ (●) derived from experiments $DC_{th} = R_{max} - R_1$ (○), and $DL_{th} = R_{max} - R_{0.001}$ (■) derived from the model for Chemistry II with a separator

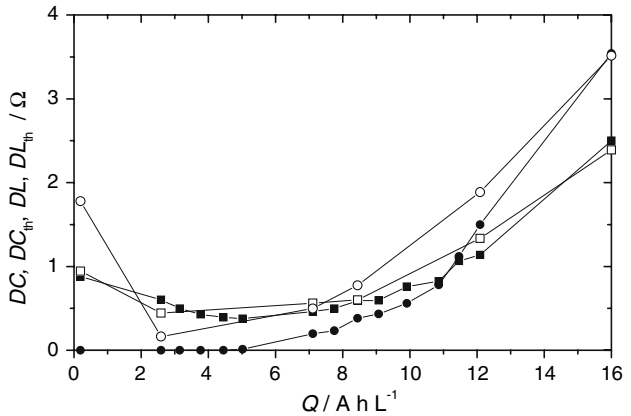

Fig. 7 Change of $DL = R_{max} - R_{0.01}$ (●) and $DC = R_{max} - R_1$ (■) derived from experiments and $DC_{th} = R_{max} - R_1$ (□), and $DL_{th} = R_{max} - R_{0.001}$ (○) derived from the model for Chemistry I with respect to the bath ageing amount

4.4 Equivalent circuit of the impedance during bath ageing

Another approach for describing the experimentally derived impedance diagrams is to devise an electrical equivalent circuit whose component values are dependent

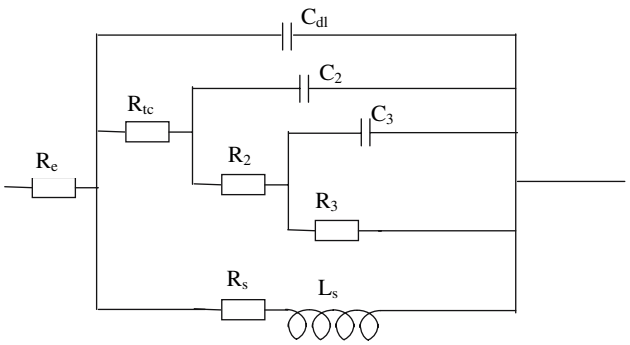

Fig. 10 Equivalent circuit used to interpret the impedance diagram measured during copper plating

on the ageing on the bath. As an example, the equivalent circuit depicted in Fig. 10 was used to quantify the evolutions of the third capacitive loop and the inductive loop diameters with respect to time for the impedance diagram obtained during ageing up to 16 A h L^{-1} for Chemistry I (see Fig. 1a–f). Figure 11 shows the change of four equivalent circuit components from Fig. 10: R_3, C_3, R_s and L_s, with time as the bath ages. All four parameters exhibit a significant variation with bath ageing, although the change is non-linear. From a theoretical point-of-view, it is difficult to interpret each equivalent circuit component in terms of the framework of a kinetic reaction mechanism. Still, the parameter variation with bath ageing might be exploited in a practical sense to follow bath ageing during the plating process.

4.5 Sensor development for plating bath ageing characterization

The experimental results and calculated parameters from the kinetic-based model and equivalent circuit analysis suggest that three methods are possible to characterize the copper plating bath ageing using electrochemical impedance measurements:

- Extract additive complexation or byproduct concentrations from the impedance diagram using the kinetic-based model,
- Calculate experimental parameters taken directly from the impedance diagram that are related to the capacitive and inductive loops, such as *DC* and *DL*,

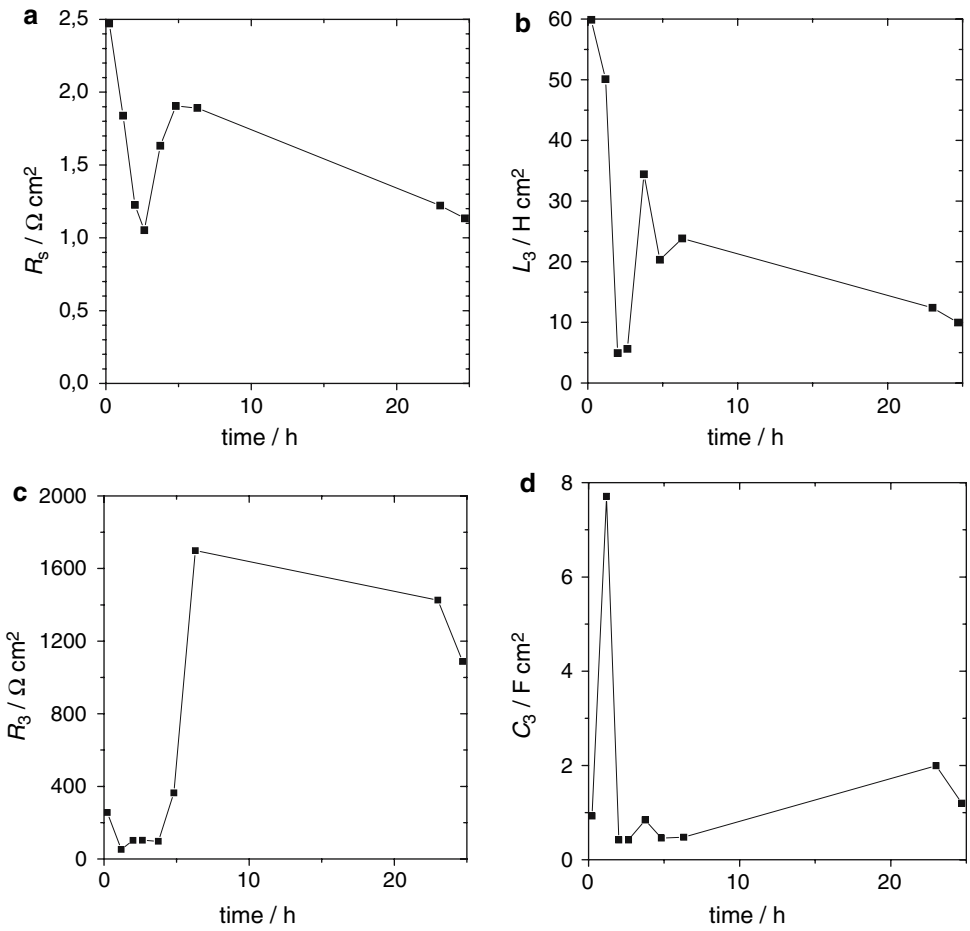

Fig. 11 Fitted values of four components, (**a**) R_s, (**b**) L_s. (**c**) R_3, (**d**) L_3, of the equivalent circuit of Fig. 10 of the electrochemical impedance measured during copper deposit in Chemistry I for ageing between 0 and 16 A h L^{-1} (Fig. 1a–f)

– Follow variations in the resistive, capacitive and inductive components calculated from an equivalent circuit model.

The choice of which method to use to further develop a practical bath ageing monitor mainly depends on the level of complexity in extracting the information in real-time during the plating process. For instance, a microcomputer is needed to fit the whole impedance diagram so that the parameters of the kinetic mechanism or the electronic components of the equivalent circuit can be calculated. On the other hand, the parameters, *DC* and *DL*, are easier to obtain using a fitting program, since only the real part of the impedance at 1, 0.01 Hz and at the maximum are needed. In addition, the use of the kinetic-based model or the equivalent circuit analysis necessitates measuring the impedance down to very low frequencies, often of the order of 0.001 Hz, in order to obtain a fit of good quality. It was noted earlier that these frequencies need a long measurement time which can be detrimental to the measurement accuracy because of drifts due to deposition and ageing during the measurement.

Thus, from a practical standpoint, a method based on calculating the experimental parameters, *DC* and *DL*, seems to be the easiest and fastest way of developing a practical monitor of copper plating bath ageing. Depending on the chemistry, either the parameter *DC* or *DL* can be chosen. Since the value of *DC* needs only a few minutes to be evaluated whereas the value of *DL* needs about 20 min, if the chemistry is such that a third capacitive loop exists, *DC* can be chosen to shorten the measurement time. If *DC* does not exist, as seen for Chemistry II without separator, *DL* has to be chosen. It is anticipated that for each new chemistry, it will be necessary to carry out a calibration procedure to determine which characteristic parameter will be used to follow bath ageing. Ultimately, the limits where the bath has to be renewed can then be determined by comparing the change in the parameter chosen to the superfilling quality of the bath during the actual copper interconnect deposition process.

5 Conclusion

The ageing of industrial copper plating baths used in integrated circuit interconnect manufacturing plating processes was followed by means of electrochemical impedance measurements. In addition, a physico-chemical model was also tested during ageing of the plating bath. It was shown that the kinetics of the industrial bath is similar in many respects to the kinetics of a reference bath whose chemistry and superfilling capabilities are well-known. Although the composition of the accelerator and inhibitor species are not specifically known, the model accounts for their presence and interaction in the bulk solution as well as on the copper surface. The slight discrepancies observed between the experimental data and the model predictions can be ascribed to possible levellers contained in the industrial bath, which is not taken into account in the model. Furthermore, the potential of impedance spectroscopy as a method to follow bath ageing was assessed by comparing the parameters obtained from the impedance diagrams using the kinetic model, an equivalent circuit model, or the characteristic impedance loop diameters. The approximate measure of the diameter of the low frequency loops was concluded to be the easiest way to devise a protocol for following bath ageing and bath renewal. By using these characteristic parameters related to the quality of the plating bath, a monitoring technique can be inferred, which could be applied to industrial production lines.

Acknowledgement The authors acknowledge the support of Altis Semiconductor, Corbeil-Essones, France on this project. In particular, special thanks to Christelle Mace, Eric Chabal and Anne Quennoy of the Cu ECD team at Altis for their help during the impedance measurements.

References

1. Moffat TP, Wheeler D, Huber WH, Josell D (2001) Electrochem Solid State Lett 4:C26
2. Koh LT, You GZ, Lim SY, Lim CY, Foo PD (2001) Microelectronics J 32:973
3. Epelboin I, Lenoir F, Wiart R (1972) J Cryst Growth 13:417
4. Burrows IR, Harrison JA, Thomson J (1975) J Electroanal Chem 58:241
5. Razumney G, O'M Bockris J (1973) J Electroanal Chem 46:185
6. Harrison JA, Thirsk HR (1971) In: Bard AJ (ed) Electroanalytical chemistry, vol 5. Marcel Dekker, New York, p 67
7. Chassaing E, Wiart R (1984) Electrochim Acta 29:649
8. Soares DM, Wasle S, Weil KG, Doblhofer K (2002) J Electroanal Chem 532:353
9. Healy JP, Pletcher D, Goodenough M (1992) J Electronal Chem 338:155
10. Gabrielli C, Moçotéguy Ph, Perrot H, Wiart R (2004) J Electroanal Chem 572:367
11. Gabrielli C, Moçotéguy Ph, Perrot H, Nieto-Senz D, Zdunek A (2006) Electrochim Acta 51:1462
12. Gabrielli C, Moçotéguy Ph, Perrot H, Nieto-Sanz D, Zdunek A (2007) J Electrochem Soc 154:D13
13. (a) Moffat TP, Bonevich JE, Huber WH, Stanishevsky A, Kelly DR, Stafford GR, Josell D (2000) J Electrochem Soc 147:4524. (b) Mattson E, O'M Bockris J (1959) Trans Faraday Soc 55:1586
14. O'M Bockris J, Enyo M (1962) Trans Faraday Soc 58:11
15. Brown OR, Thirsk HR (1965) Electrochim Acta 10:3
16. Chao F, Costa M (1968) Bull Soc Chim Fr 10:4015
17. Rashkov ST, Vuchkov L (1981) Surf Technol 14:309
18. Gabrielli C, Moçotéguy Ph, Perrot H, Zdunek A, Nieto-Sanz D, Clech MC (2003) Electrochem Soc Proc 2003:121
19. Gabrielli C, Moçotéguy PC, Perrot H, Zdunek A, Bouard P, Haddix M (2004) Electrochem Solid State Lett 7:C31